Published in final edited form as:
Biochem Biophys Res Commun. 2013 February 15; 431(3): 547–553. doi:10.1016/j.bbrc.2013.01.020.

Filamentous fungal-specific septin AspE is phosphorylated *in vivo* and interacts with actin, tubulin and other septins in the human pathogen *Aspergillus fumigatus*

Praveen Rao Juvvadi[1], **Detti Belina**[1], **Erik J. Soderblom**[3], **M. Arthur Moseley**[3], and **William J. Steinbach**[1,2,*]

[1]Division of Pediatric Infectious Diseases, Department of Pediatrics, Duke University Medical Center, Durham NC, USA

[2]Department of Molecular Genetics & Microbiology, Duke University Medical Center, Durham NC, USA

[3]Duke Proteomics Core Facility, Institute for Genome Sciences and Policy, Duke University, Durham, NC, USA

Abstract

We previously analyzed the differential localization patterns of five septins (AspAÊ), including a filamentous fungal-specific septin, AspE, in the human pathogen *Aspergillus fumigatus*. Here we utilized the *A. fumigatus* strain expressing an AspE-EGFP fusion protein and show that this novel septin with a tubular localization pattern in hyphae is phosphorylated *in vivo* and interacts with the other septins, AspA, AspB, AspC and AspD. The other major proteins interacting with AspE included the cytoskeletal proteins, actin and tubulin, which may be involved in the organization and transport of the septins. This is the first report analyzing the phosphorylation of AspE and localizing the sites of phosphorylation, and opens opportunities for further analysis on the role of post-translational modifications in the assembly and organization of *A. fumigatus* septins. This study also describes the previously unknown interaction of AspE with the actin-microtubule network. Furthermore, the novel GFP-Trap® affinity purification method used here complements widely-used GFP localization studies in fungal systems.

Keywords

Aspergillus; Septin; AspE; Phosphorylation; GFP-Trap® affinity purification; Mass spectrometry

1. Introduction

Septins are a highly conserved family of GTP-binding proteins distributed in all eukaryotes except plants and function by forming heteropolymeric structures [1,2]. In contrast to mammalian septins that are encoded by a multi-gene family comprising 12 genes (*SEPT1-12*) [1,3], the model yeast *Sacchromyces cerevisiae* contains 7 septin genes (*CDC3,*

[*]**Corresponding Author:** William J. Steinbach, Division of Pediatric Infectious Diseases, Department of Pediatrics, Duke University Medical Center, Durham, NC 27710, bill.steinbach@duke.edu, Tel: (919) 681-1504, Fax (919) 668-4859 .

CDC10, CDC11, CDC12, SHS1, SPR3 and *SPR28*) that are differentially expressed during vegetative growth and sporulation [4,5,6]. However, the filamentous group of fungi, including *Aspergillus* species, consists of 4 septins (AspA~D) that are orthologous to *S. cerevisiae* septins and a fifth septin (AspE) unique to filamentous fungi [7]. Although septins have been proposed to regulate a wide variety of functions in mammalian cells [1,2,3,8] and the yeasts [1,4,5,6,9], knowledge of their roles in filamentous fungi is limited to morphogenetic events involving hyphal branching, septation, and conidiophore development [10,11,12]. Earlier reports implicated a role for septins in tissue invasion and virulence of the pathogenic yeast *Candida albicans* [13], and recent data from the plant pathogenic filamentous fungus *Magnaporthe grisea* revealed the importance of septins for plant cell invasion [14,15]. Therefore, studies directed towards understanding septin organization and their roles in the opportunistic human pathogen *A. fumigatus* could help decipher invasive pathogenesis and lead to identification of better molecular targets to combat invasive aspergillosis in patients.

Cellular mechanisms involved in the formation of higher order septin structures and the dynamics of septin assembly still remain unknown. In mammals and the yeasts, septin organization and dynamics have been linked to post-translational modifications involving phosphorylation [3,16,17,18]. Three kinases, Elm1, Cla4 and Gin4, control septin organization in *S. cerevisiae* [19,20,21]. After Tachikawa et al [22] reported that a Gip1p-Glc7p phosphatase complex is required for proper septin organization and initiation of spore wall formation in *S. cerevisiae*, the Shs1p septin, which serves as the outer component of the septin complex, was shown to bind to the Gin4 kinase, indicating the possibility of Shs1 undergoing Gin4-mediated phosphorylation [23]. This was further strengthened by another report which indicated that the association of the septins Shs1p and Cdc11p involves some yeast-specific factor or post-translational modification [24]. Phosphorylation of the septin Cdc3p by the Cdc28 kinase was shown to be essential for proper disassembly of the septin ring [25]. Septin collar formation and septin filament assembly was also shown to require both GTP binding and Cla4-mediated phosphorylation of septins [24]. Furthermore, Dobbelaere et al [17] showed that RTS1 (the regulatory subunit of protein phosphatase-2A) mediated dephosphorylation of septins and is required for the disassembly process, indicating that activation of septin dynamics by phosphorylation events controls the rigidity of the septin ring.

Although these results indicated that phosphorylation and dephosphorylation regulate septin architecture in the yeasts, there is limited information on the analysis of septin interactions and phosphorylation in filamentous fungi. Only recently in *Ashbya gossypii*, a filamentous fungus belonging to the saccharomycotina subphyla and closely related to yeast, the assembly of a subset of septin rings was shown to be associated with two kinases, Elm1p and Gin4p [26]. Multiple phosphorylation sites were identified in the *A. gossypii* septin, Shs1p [27], and also the other septins [28]. Although mutation of Shs1p phosphorylable sites led to decreased septin dynamics, phosphomimetic mutations were lethal [28], revealing a dynamic regulation of septin organization by phosphorylation /dephosphorylation mechanisms. While *A. gossypii* belongs to the filamentous group of fungi, it lacks the ortholog of AspE which is present in pezizomycota, the largest subphyla of filamentous fungi.

We previously reported the differential localization patterns of all the 5 septins in the human pathogenic fungus *A. fumigatus*, and showed that the filamentous fungal-specific septin, AspE, localized as long tubular or filament-like structures which were disrupted in presence of actin and microtubule inhibitors [29]. In order to further understand the mechanism of AspE assembly in the septin complex, here we purified the AspE-GFP fusion protein to identify its interactants and also examine its phosphorylation status *in vivo*. We show that

AspE interacted with all of the other 4 septins (AspA, AspB, AspC and AspD) as well as the other major binding proteins, actin and tubulin. In addition, we also show for the first time that AspE is highly phosphorylated at the N-terminus, within the G-domain, and at its C-terminal region, indicating the possible role for phosphorylation in the assembly of *A. fumigatus* septins.

2. Materials and methods

2. 1. Organism and culturing, Protein extraction and AspE-GFP purification

The *A. fumigatus* strain expressing the *aspE-egfp* fusion construct under the control of the *otef* promoter was grown in glucose minimal media (GMM) liquid medium as a shaking culture for 24 h at 37°C. Total cell lysate was extracted by homogenizing the fungal tissue (1.5~2 mg wet weight) using liquid nitrogen and suspended in 5 ml lysis buffer (10 mM Tris-HCl pH 7.5, 150 mM NaCl, 0.5 mM EDTA, 0.01% Triton X-100, 1mM DTT, 1mM PMSF, 1:100 Protease Inhibitory Cocktail) and centrifuged at 5000 rpm for 10 min at 4°C to remove cell debris. The crude supernatant was clarified by centrifugation at 7000 rpm for 15 min at 4°C. Total protein in the crude extract was quantified by Bradford method and normalized to contain ~10 mg protein in the sample before GFP-Trap® affinity purification (Chromotek). GFP-Trap® resin (35 μl) was equilibrated by washing three times in 500 μl ice-cold dilution buffer (10 mM Tris-HCl pH 7.5, 150 mM NaCl, 0.5 mM EDTA, 1mM PMSF, 1:100 Protease Inhibitory Cocktail) according to the manufacturer instructions and finally resuspended in 100 μl ice cold dilution buffer. The GFP-Trap® resin suspension was then mixed with total crude cell lysate containing ~10 mg total protein and incubated at 4°C by gentle agitation for 2 h. The suspension was centrifuged at 2000 rpm for 10 min at 4°C and the pelleted GFP-Trap® resin was washed once in 500 μl of ice-cold dilution buffer and then twice with 500 μl of wash buffer (10 mM Tris-HCl pH 7.5, 350 mM NaCl, 0.5 mM EDTA, 1mM PMSF, 1:100 Protease Inhibitory Cocktail).

2.3. Sample Preparation and Nano-Flow Liquid Chromatography Electrospray Ionization Tandem Mass Spectrometry (LC-MS/MS) Analysis

Protein bound GFP-Trap® resins were washed three times with 50 mM ammonium bicarbonate, pH 8.0, and then suspended in 30 μl 50 mM ammonium bicarbonate, pH 8.0, supplemented with 0.1% Rapigest SF surfactant (Waters Corp). Samples were reduced with 5 mM dithiolthreitol for 30 min at 70°C and free sulfhydryls were alkylated with 10 mM iodoacetamide for 45 min at room temperature. Proteolytic digestion was accomplished by the addition of 500 ng sequencing grade trypsin (Promega) directly to the resin with incubation at 37°C for 18 hours. Supernatants were collected following a 2 min centrifugation at 1,000 rpm, acidified to pH 2.5 with TFA, and incubated at 60°C for 1 h to hydrolyze the remaining Rapigest surfactant. Insoluble hydrolyzed surfactant was cleared by centrifugation at 15,000 rpm for 5 min. Ninety percent (by volume) of the sample was then removed for subsequent phosphopeptide analysis and the remaining ten percent (by volume) was subjected to an unbiased protein interaction analysis. For the phosphopeptide analysis, samples were dried using vacuum centrifugation and resuspended in 100 μl 80% acetonitrile, 1% TFA, 50 mg/mL MassPrep Enhancer, pH 2.5 (Waters Corp). Peptides were subjected to phosphopeptide enrichment using a 200 μL TiO_2 Protea Tip (Protea Bio) and subsequently washed with 200 μl 80% acetonitrile, 1% TFA, 50 mg/ml MassPrep Enhancer followed by 200 μl 80% acetonitrile, 1% TFA. Peptides were eluted in 50 μl 20% acetonitrile, 5% aqueous ammonia, pH 10.5 and then acidified to pH 2.5 with formic acid prior to drying using vacuum centrifugation.

Samples were resuspended in 10 μl 2% acetonitrile, 0.1% formic acid and subjected to chromatographic separation on a Waters NanoAquity UPLC equipped with a 1.7 μm

BEH130 C_{18} 75 μm I.D. × 250 mm reversed-phase column. Phosphopeptide enriched samples were additionally supplemented with 10 mM citric acid. The mobile phase consisted of (A) 0.1% formic acid in water and (B) 0.1% formic acid in acetonitrile. Following a 5 μl injection, peptides were trapped for 5 min on a 5 μm Symmetry C_{18} 180 μm I.D. × 20 mm column at 20μl/min in 99.9% A. The analytical column was held at 5% B for 5 min then switched in-line and a linear elution gradient of 5% B to 40% B was performed over 90 min at 300 nl/min. The analytical column was connected to a fused silica PicoTip emitter (New Objective, Cambridge, MA) with a 10 μm tip orifice. Phosphopeptide enriched samples were analyzed on an LTQ-Orbitrap XL mass spectrometer with a precursor MS scan in the Orbitrap from *m/z* 400-2000 with r = 60,000 at *m/z* 400 and a target AGC setting of 1e6 ions. In a data-dependent mode of acquisition, MS/MS spectra of the three most abundant precursor ions were acquired in the linear ion-trap with a target AGC setting of 1e3 ions. Max fill times were set to 1000 ms for full MS scans and 250 ms for MS/MS scans with minimum MS/MS triggering thresholds of 5000 counts. For all experiments, fragmentation occurred in the LTQ linear ion trap with a CID energy setting of 35% and a dynamic exclusion of 60 s was employed for previously fragmented precursor ions. For unbiased protein interaction studies, data were acquired on a Waters Synapt G2 mass spectrometer with precursor MS scans from *m/z* 50-2000 operating in a data-dependent mode of acquisition. The top three most abundant ions were selected for MS/MS using a charge state dependent CID energy setting with a 60s dynamic exclusion list employed.

2.4. Data analysis

Raw LC-MS/MS data files were processed in Mascot distiller (Matrix Science) and then submitted to independent Mascot database searches (Matrix Science) against a NCBI fungus entry. database (download date; Feb 18, 2012) appended with the reverse sequence of each forward entry. Search tolerances were 10 ppm for precursor ions and either 0.8 Da or 0.04 Da for product ions for LTQ-Orbitrap XL or Synapt G2 data, respectively, using trypsin specificity with up to two missed cleavages. Carbamidomethylation (+57.0214 Da on C) was set as a fixed modification, whereas oxidation (+15.9949 Da on M) and phosphorylation (+79.9663 Da on S, T, and Y) were considered a variable modifications. All searched spectra were imported into Scaffold (v 3.6.2, Proteome Software) and confidence thresholds were set using a Bayesian statistical algorithm based on the PeptideProphet and ProteinProphet algorithms which yielded a peptide and protein false discovery rate of 0% [30,31]. Only those proteins with at least two unique peptides to match were considered as being correct. Phosphorylation site localization was assessed by exporting peak lists directly from Scaffold into the online AScore algorithm (http://ascore.med.harvard.edu/ascore.html) [32]. A scaffold file containing the raw data is available for download here: https://discovery.genome.duke.edu/express/resources/3339/AspE_Phosphorylation_Interation.sf3

3. Results and Discussion

3.1. AspE interacts with actin-microtubule network and rest of the septin complex

We previously noted that, in contrast to AspA, AspB, AspC and AspD (the core septin homologs of cdc11p, cdc3p, cdc12p and cdc10p), the filamentous fungal-specific septin AspE showed filament-like tubular localization pattern along the *A. fumigatus* hyphae. Drugs that inhibit actin polymerization and microtubule stability mislocalized AspE from filaments to dot-like structures, which were presumed to be Microtubule Organizing Centers (MTOCs) [29]. Previous studies with mammalian septins have revealed the importance of actin and microtubules in the organization of septins [2]. In order to investigate if AspE interacted with the cytoskeletal proteins and the whole septin complex *in vivo*, we utilized the *A. fumigatus* strain expressing AspE-EGFP fusion protein to purify the AspE protein-

complex by exploiting the EGFP-tag that bound to the GFP-Trap® agarose resin; bound proteins were directly subjected to LC-MS after proteolytic digestion. As shown in Table 1, a total of 48 proteins were identified with at least 2 unique peptides to match. The top identified protein was AspE with 40 unique peptides to match and with 63% sequence coverage. All of the other septins (AspB, AspD, AspA and AspC) were identified as AspE-binding partners along with other major proteins, including actin, tubulin (beta chain, alpha-1 subunit, beta subunit), Hsp70 chaperone, and translational elongation factor subunits (EF-1 and EF-2). Previously, the interaction of the mammalian septin, Sept6p, with non-septin binding partners, including Hsp70 and Hsp70-like proteins, was shown but significance of these interactions was not studied further [33]. Apart from ribosomal proteins, we also identified some metabolic-related enzymes such as phosphoglycerate kinase, isocitrate dehydrogenase, succinyl-CoA synthetase and calmodulin-dependent protein kinase as AspE binding proteins.

3.2. Phosphorylation of AspE occurs in the polybasic region, G-domain and the C terminal end

Earlier reports in *S. cerevisiae* have shown that phosphorylation of cdc3p regulates the ratio between septin rings and unbound monomeric septin [25], and phosphorylation of cdc10p and shs1p regulate septin collar formation and the fluidity of the septin ring at the bud neck, respectively [9,17,23,24]. A recent report analyzing septin phosphorylations and mutation of the phosphorylatable residues from *A. gossypii* also showed that phosphorylation plays a key role in septin organization [28]. Because there are no data available on phosphorylation of septins in any *Aspergillus* species [16], coupled with the probability of phosphorylation resulting in the formation of higher ordered septin structures, we were interested in examining the phosphorylation status of the *A. fumigatus* septins. To accomplish this, the AspE-GFP purified protein complex was subjected to phosphopeptide enrichment and the sample was subjected to LC-MS/MS to identify the specific phosphorylation sites on AspE. As shown in Table 2, a total of 6 phosphorylation sites were detected in 5 unique phosphorylated peptides. All of the phosphorylated residues in AspE were serines, located at positions Ser48, Ser209, Ser283, Ser430, Ser434 and Ser533. An example annotated MS/MS spectrum of the doubly phosphorylated peptide AEVS*PPGS*PSQR is shown in Figure 1A with the corresponding fragment ion coverage table. Selected ion chromatogram traces of the intact precursor ion (Figure 1B) illustrate a single peak at retention time ~20.5 min. As localization of the phosphorylation modification cannot be directly assessed by Mascot ion scores alone, each of these peptides were subjected to AScore scoring, a site localization probability algorithm publically available at http://ascore.med.harvard.edu/ascore.html [32]. The results indicated high confidence localizations (>99%) for all 6 of the phosphorylated residues (Table 2). As shown in Fig. 2, while Ser48 is present in the N-terminal polybasic domain and the Ser533 is at the C-terminus just after the septin unique element (SUE), 2 phosphorylated residues (Ser209 and Ser283) were present between the G1 and G3 domains. Two other sites, Ser430 and Ser434, were close to each other and resided between G4 domain and the SUE.

3.3. Conservation of the AspE phosphorylated residues among Aspergillus species

Although AspE from different *Aspergillus* species is highly conserved in the G domain, the N and C-terminal regions are variable (Fig. 3). Among the 6 phosphorylation sites detected, 4 sites were conserved at positions Ser48, Ser283, Ser434 and Ser533. The polybasic region in the N-terminus is thought to be involved in membrane interaction of septin filaments through phosphatidylinositol-4,5-bisphosphate (PIP2) binding and the presence of PIP2 promoted filament assembly and organization [34]. It is therefore possible that phosphorylation of the conserved Ser48 residue within the polybasic region is involved in membrane association of AspE. Moreover, the phosphorylation we observed at the

conserved Ser533 site in the divergent C-terminus may also be very significant for AspE filamentation because phosphorylations occurring in the N and C termini of the core septins (cdc3p, cdc10p, cdc11p and cdc12p) are known to regulate the assembly and disassembly of the septin ring [16]. As shown in Fig. 2, only one (Ser283) of the two phosphorylation sites (Ser209 and Ser283) within the G1 and G3 motifs is conserved. Between the G4 motif and S4 motif, phosphorylation occurred at a short serine-proline rich region on the Ser430 and Ser434, but only Ser434 was conserved among different Aspergilli (Fig. 3). While further experiments are required to understand the significance of these phosphorylation sites in AspE, it is possible that more than one kinase is responsible for the phosphorylation of the 6 serine residues we identified. Ser430 and Ser434 are present in a short proline-rich domain that could be a target of proline-directed kinases. The sequence 45RAKSTEPLS53 in which Ser48 was phosphorylated resembles the consensus site (RXXS/T) of phosphorylation by a calmodulin dependent protein kinase [35], and it is interesting to note that calmodulin dependent protein kinase was identified as an AspE interacting protein (Table 1). Further mutational analyses of these individual residues to either non-phosphorylable or phosphomimetic residues would reveal their specific roles in the localization of AspE to filaments, and as well as their role in the organization or assembly of the whole septin complex. Additionally, analyzing the phosphorylation status of the other septins in *A. fumigatus* would also be helpful because specific alterations in individual septin phosphorylation sites can result in severe cell defects [28]. Further studies directed towards deletion of the *A. fumigatus* septin genes and understanding the importance of post-translational modifications for their organization will be useful for future antifungal drug design and targeting.

Acknowledgments

This work was supported by 1R21AI097541-01A1 from the NIH/NIAID to WJS.

Abbreviations

GFP	green fluorescent protein
Asp	*Aspergillus* septin
LC-MS/MS	Liquid Chromatography Electrospray Ionization Tandem Mass Spectrometry

References

[1]. Cao L, Yu W, Wu Y, Yu L. The evolution, complex structures and function of septin proteins. Cellular and Molecular Life Sciences. 2009; 66:3309–3323. [PubMed: 19597764]

[2]. Mostowy S, Cossart P. Septins: the fourth component of the cytoskeleton. Nat Rev Mol Cell Biol. 2012; 13:183–194. [PubMed: 22314400]

[3]. Kinoshita M. Assembly of Mammalian Septins. Journal of Biochemistry. 2003; 134:491–496. [PubMed: 14607974]

[4]. Oh Y, Bi E. Septin structure and function in yeast and beyond. Trends in Cell Biology. 2011; 21:141–148. [PubMed: 21177106]

[5]. Fares H, Goetsch L, Pringle JR. Identification of a developmentally regulated septin and involvement of the septins in spore formation in Saccharomyces cerevisiae. The Journal of Cell Biology. 1996; 132:399–411. [PubMed: 8636217]

[6]. Onishi M, Koga T, Hirata A, Nakamura T, Asakawa H, Shimoda C, Bähler J, Wu J-Q, Takegawa K, Tachikawa H, Pringle JR, Fukui Y. Role of Septins in the Orientation of Forespore Membrane Extension during Sporulation in Fission Yeast. Molecular and Cellular Biology. 2010; 30:2057–2074. [PubMed: 20123972]

[7]. Pan F, Malmberg R, Momany M. Analysis of septins across kingdoms reveals orthology and new motifs. BMC Evolutionary Biology. 2007; 7:103. [PubMed: 17601340]

[8]. Saarikangas J, Barral Y. The emerging functions of septins in metazoans. EMBO Rep. 2011; 12:1118–1126. [PubMed: 21997296]

[9]. Garcia G, Bertin A, Li Z, Song Y, McMurray MA, Thorner J, Nogales E. Subunit-dependent modulation of septin assembly: Budding yeast septin Shs1 promotes ring and gauze formation. The Journal of Cell Biology. 2011; 195:993–1004. [PubMed: 22144691]

[10]. Gladfelter AS. Guides to the final frontier of the cytoskeleton: septins in filamentous fungi. Current Opinion in Microbiology. 2010; 13:720–726. [PubMed: 20934902]

[11]. Hernández-Rodríguez Y, Hastings S, Momany M. The Septin AspB in Aspergillus nidulans Forms Bars and Filaments and Plays Roles in Growth Emergence and Conidiation. Eukaryotic Cell. 2012; 11:311–323. [PubMed: 22247265]

[12]. Lindsey R, Cowden S, Hernández-Rodríguez Y, Momany M. Septins AspA and AspC Are Important for Normal Development and Limit the Emergence of New Growth Foci in the Multicellular Fungus Aspergillus nidulans. Eukaryotic Cell. 2010; 9:155–163. [PubMed: 19949047]

[13]. L L, González-Novo A, Jiménez A, Sánchez-Pérez M, Jiménez J. Role of the septin Cdc10 in the virulence of Candida albicans. Microbiol Immunol. 2006; 50:499–511. [PubMed: 16858141]

[14]. Dagdas YF, Yoshino K, Dagdas G, Ryder LS, Bielska E, Steinberg G, Talbot NJ. Septin-Mediated Plant Cell Invasion by the Rice Blast Fungus, Magnaporthe oryzae. Science. 2012; 336:1590–1595. [PubMed: 22723425]

[15]. Saunders DGO, Dagdas YF, Talbot NJ. Spatial Uncoupling of Mitosis and Cytokinesis during Appressorium-Mediated Plant Infection by the Rice Blast Fungus Magnaporthe oryzae. The Plant Cell Online. 2010; 22:2417–2428.

[16]. Hernández-Rodríguez Y, Momany M. Posttranslational modifications and assembly of septin heteropolymers and higher-order structures. Current Opinion in Microbiology. 2012; 15:660–668. [PubMed: 23116980]

[17]. Dobbelaere J, Gentry MS, Hallberg RL, Barral Y. Phosphorylation-Dependent Regulation of Septin Dynamics during the Cell Cycle. Developmental Cell. 2003; 4:345–357. [PubMed: 12636916]

[18]. Sinha I, Wang Y-M, Philp R, Li C-R, Yap WH, Wang Y. Cyclin-Dependent Kinases Control Septin Phosphorylation in Candida albicans Hyphal Development. Developmental Cell. 2007; 13:421–432. [PubMed: 17765684]

[19]. Cvrcková F, De Virgilio C, Manser E, Pringle JR, Nasmyth K. Ste20-like protein kinases are required for normal localization of cell growth and for cytokinesis in budding yeast. Genes & Development. 1995; 9:1817–1830. [PubMed: 7649470]

[20]. Longtine MS, Fares H, Pringle JR. Role of the Yeast Gin4p Protein Kinase in Septin Assembly and the Relationship between Septin Assembly and Septin Function. The Journal of Cell Biology. 1998; 143:719–736. [PubMed: 9813093]

[21]. Bouquin N, Barral Y, Courbeyrette R, Blondel M, Snyder M, Mann C. Regulation of cytokinesis by the Elm1 protein kinase in Saccharomyces cerevisiae. Journal of Cell Science. 2000; 113:1435–1445. [PubMed: 10725226]

[22]. Tachikawa H, Bloecher A, Tatchell K, Neiman AM. A Gip1p-Glc7p phosphatase complex regulates septin organization and spore wall formation. The Journal of Cell Biology. 2001; 155:797–808. [PubMed: 11724821]

[23]. Mortensen EM, McDonald H, Yates J, Kellogg DR. Cell Cycle-dependent Assembly of a Gin4-Septin Complex. Molecular Biology of the Cell. 2002; 13:2091–2105. [PubMed: 12058072]

[24]. Versele M, Thorner J. Septin collar formation in budding yeast requires GTP binding and direct phosphorylation by the PAK, Cla4. The Journal of Cell Biology. 2004; 164:701–715. [PubMed: 14993234]

[25]. Tang CS RS. Phosphorylation of the Septin Cdc3 in G1 by the Cdc28 Kinase Is Essential for Efficient Septin Ring Disassembly. Cell Cycle. 2002; 1:38–45.

[26]. DeMay BS, Meseroll RA, Occhipinti P, Gladfelter AS. Regulation of Distinct Septin Rings in a Single Cell by Elm1p and Gin4p Kinases. Molecular Biology of the Cell. 2009; 20:2311–2326. [PubMed: 19225152]

[27]. Meseroll RA, Howard L, Gladfelter AS. Septin ring size scaling and dynamics require the coiled-coil region of Shs1p. Molecular Biology of the Cell. 2012; 23:3391–3406. [PubMed: 22767579]

[28]. Meseroll RA, Occhipinti P, Gladfelter AS. Septin phosphorylation and coiled-coil domains function in cell and septin ring morphology in the filamentous fungus Ashbya gossypii. Eukaryotic Cell. 2012

[29]. Juvvadi PR, Fortwendel JR, Rogg LE, Steinbach WJ. Differential localization patterns of septins during growth of the human fungal pathogen Aspergillus fumigatus reveal novel functions. Biochemical and Biophysical Research Communications. 2011; 405:238–243. [PubMed: 21219860]

[30]. Keller A, Nesvizhskii AI, Kolker E, Aebersold R. Empirical Statistical Model To Estimate the Accuracy of Peptide Identifications Made by MS/MS and Database Search. Analytical Chemistry. 2002; 74:5383–5392. [PubMed: 12403597]

[31]. Nesvizhskii AI, Keller A, Kolker E, Aebersold R. A Statistical Model for Identifying Proteins by Tandem Mass Spectrometry. Analytical Chemistry. 2003; 75:4646–4658. [PubMed: 14632076]

[32]. Beausoleil SA, Villen J, Gerber SA, Rush J, Gygi SP. A probability-based approach for high-throughput protein phosphorylation analysis and site localization. Nat Biotech. 2006; 24:1285–1292.

[33]. Kremer BE, Haystead T, Macara IG. Mammalian Septins Regulate Microtubule Stability through Interaction with the Microtubule-binding Protein MAP4. Molecular Biology of the Cell. 2005; 16:4648–4659. [PubMed: 16093351]

[34]. Bertin A, McMurray MA, Thai L, Garcia G Iii, Votin V, Grob P, Allyn T, Thorner J, Nogales E. Phosphatidylinositol-4,5-bisphosphate Promotes Budding Yeast Septin Filament Assembly and Organization. Journal of Molecular Biology. 2010; 404:711–731. [PubMed: 20951708]

[35]. Braun AP, Schulman H. The Multifunctional Calcium/Calmodulin-Dependent Protein Kinase: From Form to Function. Annual Review of Physiology. 1995; 57:417–445.

Highlights

- *In vivo* interactions of the novel septin AspE were identified by GFP-Trap® affinity purification
- Septins AspA, AspB, AspC and AspD interacted with AspE *in vivo*
- Actin and tubulin interacted with AspE *in vivo*
- AspE is phosphorylated at 6 serine residue *in vivo*

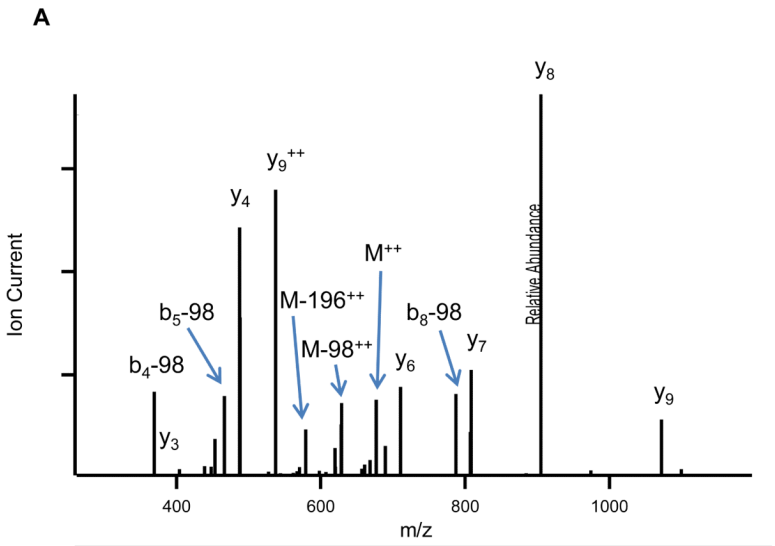

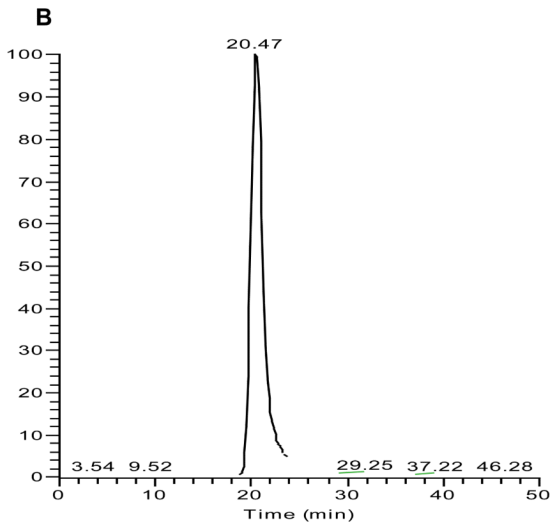

B	B Ions	B+2H	B-NH3	B-H2O	AA	Y Ions	Y+2H	Y-NH3	Y-H2O	Y
1	72.0				A	1,371.5	686.3	1,354.5	1,353.5	12
2	201.1			183.1	E	1,300.5	650.8	1,283.5	1,282.5	11
3	300.2			282.1	V	1,171.5	586.2	1,154.4	1,153.4	10
4	467.2			449.1	S+80	1,072.4	536.7	1,055.4	1,054.4	9
5	564.2			546.2	P	905.4	453.2	888.4	887.4	8
6	661.3	331.1		643.2	P	808.3	404.7	791.3	790.3	7
7	718.3	359.6		700.3	G	711.3	356.1	694.3	693.3	6
8	885.3	443.1		867.3	S+80	654.3		637.2	636.3	5
9	982.3	491.7		964.3	P	487.3		470.2	469.3	4
10	1,069.4	535.2		1,051.4	S	390.2		373.2	372.2	3
11	1,197.4	599.2	1,180.4	1,179.4	Q	303.2		286.2		2
12	1,371.5	686.3	1,354.5	1,353.5	R	175.1		158.1		1

Fig. 1.

(A) Annotated MS/MS spectrum of the doubly phosphorylated peptide AEVS*PPGS*PSQR identified within AspE following TiO_2 enrichment and high-resolution LC-MS/MS analysis. (B) Extracted ion chromatogram of m/z 686.2700 +/−10ppm, corresponding to the doubly charged precursor ion of AEVS*PPGS*PSQR, resulted in a single chromatographic elution profile at 27.5 min.

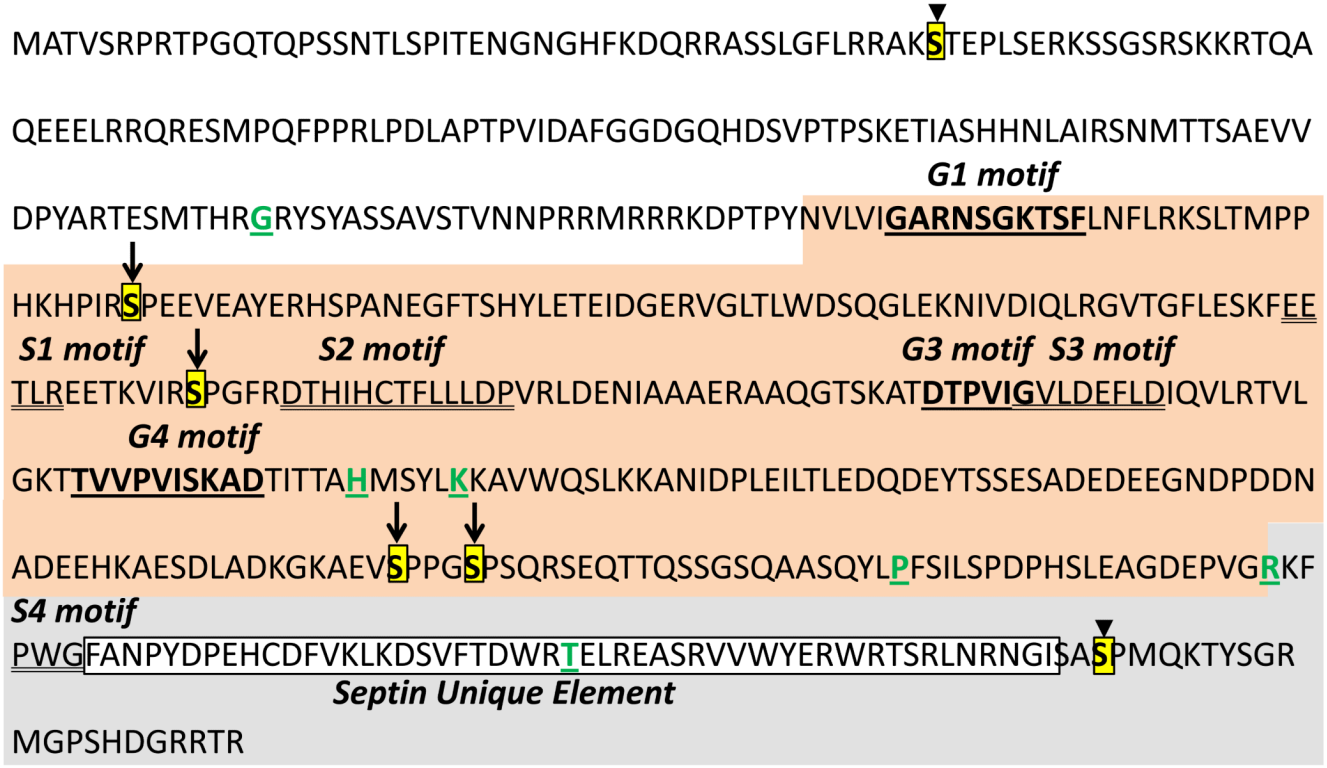

Fig. 2.

Septin AspE sequence showing various domains and sites of phosphorylations. *Aspergillus fumigatus* AspE amino acid sequence showing the 3 major domains including the N-terminus, the G-domain (in orange) and the C-terminus (in grey). The respective G-motifs (G1, G3 and G4) are underlined and in bold red color. The phosphorylated serine residues are boxed in yellow. Arrows indicate the phosphorylated residues within the G-domain and arrow heads indicate the phosphorylated residues in the N and C-termini. The septin specific motifs (S1, S2, S3 and S4) are double underlined. The other conserved single amino acid residues are indicated in green and underlined. The Septin Unique Element at the C-terminus is boxed. All the motifs were assigned based on Pan et al [7].

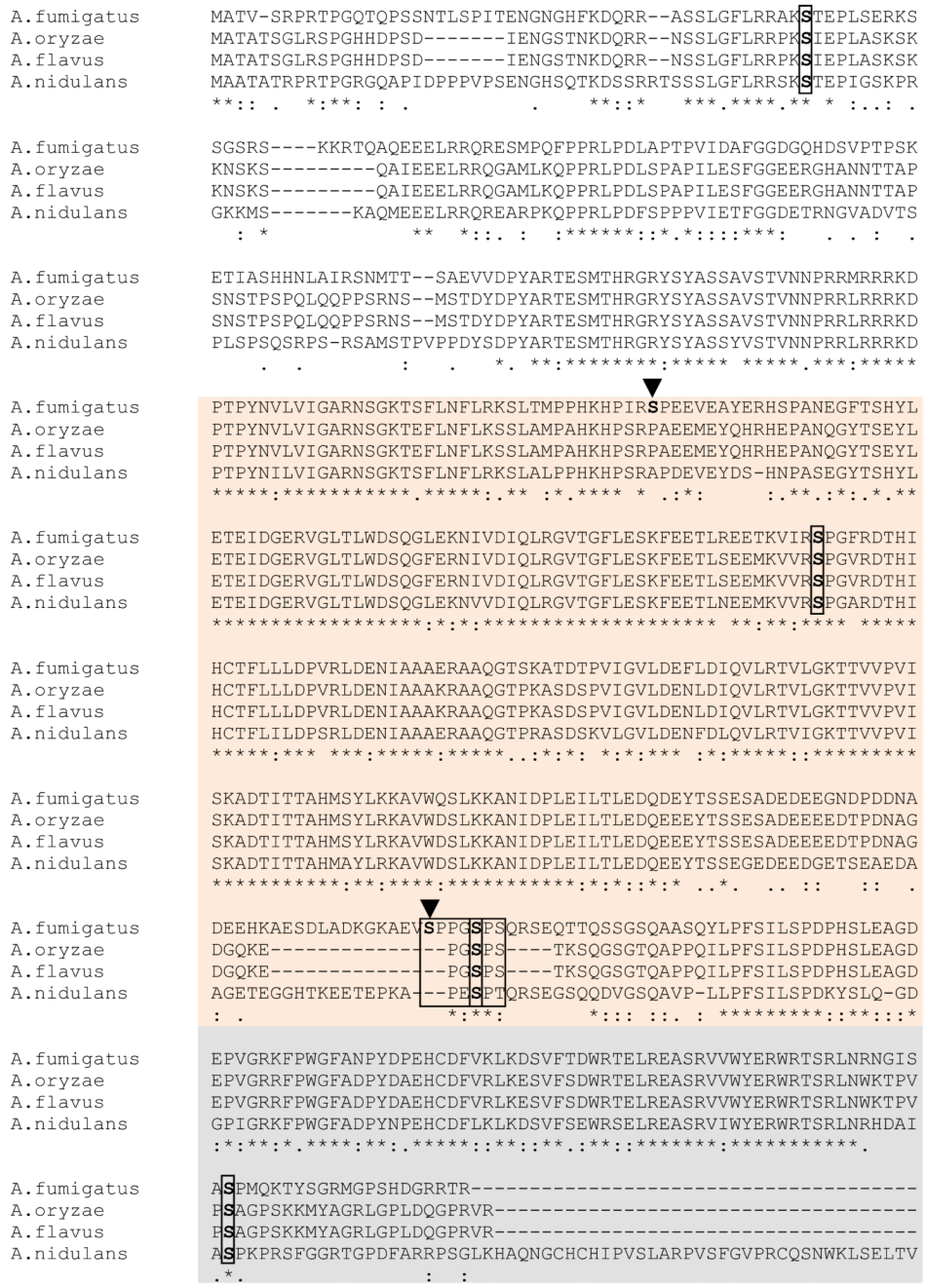

Fig. 3.

Clustal alignment of AspE homologs from other *Aspergillus* species showing conservation of phosphorylated residues. AspE homologs from other *Aspergillus* species were aligned using the ClustalW program. The sites of conserved phosphorylated residues are boxed and indicated in red color. The non-conserved phosphorylated residues are indicated by arrowheads. The short serine-proline rich region is boxed in red. The N terminal (in white) and C terminal domains (in grey) and the G-domain (in orange) are shown.

Table 1

Protein	NCBI accession number	Molecular weight (kDa)	Identified peptides
Septin Proteins			
AspE	gi|71000419	62	40
AspB	gi|70986973	59	13
AspD	gi|70994952	39	10
AspA	gi|119479605	43	8
AspC	gi|70985058	44	7
Proteins related to cytoskeleton organization			
Actin	gi|115386236	40	11
Tubulin beta chain	gi|119495802	50	8
Tubulin alpha-1 subunit	gi|70990312	50	9
Tubulin beta subunit	gi|70982752	50	4
Tubulin TubB subunit	gi|71002302	50	3
Proteins related to heat shock			
Hsp70 chaperone (HscA)	gi|70983346	67	10
Heat shock 70 kDa protein	gi|115385867	70	5
Mitochondrial Hsp70 chaperone (Ssc70)	gi|159129408	72	3
Heat shock protein 60, mitochondrial precursor	gi|115443330	62	2
Proteins related to protein synthesis and folding			
Translation elongation factor EF-1 alpha subunit	gi|146322501	54	8
Translation elongation factor EF-2 subunit	gi|71002010	93	8
40S Ribosomal protein S3	gi|70990926	29	5
40S Ribosomal protein S14	gi|115384692	16	4
Ribosomal protein S5	gi|119488785	28	4
T-complex protein 1, theta subunit	gi|119500564	61	4
Eukaryotic Translation initiation factor 4	gi|71000162	46	4
T-complex protein 1, gamma subunit	gi|115391547	57	3
Ribosomal protein S13	gi|154280018	17	3
40S Ribosomal protein S7	gi|115396282	23	2
40S Ribosomal protein S27	gi|115402529	9	2
40S Ribosomal protein S5-A	gi|119186515	24	2
Ribosomal protein S13p/S18e	gi|119473095	18	2
40S Ribosomal protein S16	gi|115384680	16	2
60S Ribosomal protein L12	gi|119497097	18	2
40S Ribosomal protein S17	gi|116194718	17	2
40S Ribosomal protein S20	gi|115398580	15	2
40S Ribosomal protein S3aE	gi|115438592	29	2
60S Ribosomal protein L4	gi|119498945	41	2

Protein	NCBI accession number	Molecular weight (kDa)	Identified peptides
T-complex protein 1, zeta subunit	gi|119195049	59	2
Proteins related to metabolism			
Alcohol dehydrogenase	gi|159126256	37	11
Bifunctional pyrimidine biosynthesis protein	gi|70992333	248	6
Phosphoglycerate kinase (pgkA)	gi|119495924	45	6
Putative flavohaemoglobin	gi|50788082	46	5
Isocitrate dehydrogenase LysB	gi|119468338	38	4
Isocitrate dehydrogenase, NAD-dependent	gi|119495397	42	4
Succinyl–CoA synthetase beta subunit	gi|119486728	48	3
ATP synthase alpha chain (mitochondrial)	gi|340521314	59	3
ATP synthase beta chain (mitochondrial)	gi|115401284	54	3
S-adenosylmethionine synthetase	gi|119495861	42	2
5-oxo-L-prolinase	gi|159130239	139	2
Homocitrate synthase (mitochondrial)	gi|115492729	51	2
Isocitrate dehydrogenase subunit 1 (mitochondrial)	gi|115400882	42	2
Calmodulin dependent protein kinase	gi|119481599	46	2

Table 2

Unique Phosphopeptide	Phosphorylated Residue	Mascot Ion Score	Ascore[1]	Localized[2]
AKS*TEPLSER	S48	40.5	24.4	Yes
S*PEEVEAYER	S209	31.0	65.5	Yes
VIRS*PGFR	S283	28.4	Unambiguous	Yes
AEVS*PPGS*PSQR	S430, S434	62.9	24.8, 38.5	Yes, Yes
NGISAS*PMQK	S533	31.3	51.6	Yes

Unique phosphorylated residues within AspE identified by TiO2-based phosphoenrichment followed by LC-MS/MS analysis.

[1] AScore phosphorylation localization score reported from http://ascore.med.harvard.edu/.

[2] Ascore values >20 indicate greater than 99% chance of correct localization versus other phosphorylatable residues.